Cell and Tissue Research (2019) 378:301–317
https://doi.org/10.1007/s00441-019-03058-y

REGULAR ARTICLE

Dietary DHA/EPA supplementation ameliorates diabetic nephropathy by protecting from distal tubular cell damage

Marija Vitlov Uljević[1] · Kristina Starčević[2] · Tomislav Mašek[3] · Ivana Bočina[4] · Ivana Restović[5] · Nives Kević[4] · Anita Racetin[6] · Genia Kretzschmar[1] · Maximilian Grobe[1] · Katarina Vukojević[1,6] · Mirna Saraga-Babić[6] · Natalija Filipović[1]

Received: 5 February 2019 / Accepted: 12 June 2019 / Published online: 29 June 2019

Abstract

The aim was to explore the influence of experimental diabetes mellitus type 1 (DM1) and potential protective/deleterious effects of different dietary n−6/n−3 PUFA ratios on renal phospholipid composition and pathological changes caused by DM1. Male Wistar rats were injected with 55 mg/kg streptozotocin or citrate buffer (control group). Control (C) and diabetic groups (STZ) were fed with n−6/n−3 ratio of ≈ 7, STZ + N6 with n−6/n−3 ratio ≈ 60 and STZ + DHA with n−6/n−3 ratio of ≈ 1 containing 16% EPA and 19% DHA. Tissues were harvested 30 days after DM1 induction. Blood and kidneys were collected and analysed for phospholipid fatty acid composition, pathohystological changes, ectopic lipid accumulation and expression of VEGF, NF-kB and special AT-rich sequence-binding protein-1 (SATB1). Pathological changes were studied also by using transmission electron microscopy, after immunostaining for VEGF. Substantial changes in renal phospholipid fatty acid composition resulted from DM1 and dietary PUFA manipulation. Extensive vacuolization of distal tubular cells (DTCs) was found in DM1, but it was attenuated in the STZ + DHA group, in which the highest renal NF-kB expression was observed. The ectopic lipid accumulation was observed in proximal tubular cells (PTCs) of all diabetic animals, but it was worsened in the STZ + N6 group. In DM1, we found disturbance of VEGF-transporting vesicular PTCs system, which was substantially worsened in STZ + DHA and STZ + N6. Results have shown that the early phase of DN is characterized with extent damage and vacuolization of DTCs, which could be attenuated by DHA/EPA supplementation. We concluded that dietary fatty acid composition can strongly influence the outcomes of DN.

Keywords Diabetic nephropathy · PUFA · Distal tubules · SATB1 · VEGF

✉ Natalija Filipović
natalija.filipovic@mefst.hr

[1] Department of Anatomy, Histology and Embryology, Laboratory for Neurocardiology, University of Split School of Medicine, Šoltanska 2, 21000 Split, Croatia

[2] Department for Forensic and State Veterinary Medicine, Laboratory for Forensic Molecular Biology, University of Zagreb Faculty of Veterinary Medicine, Zagreb, Croatia

[3] Department of Animal Nutrition and Dietetics, University of Zagreb Faculty of Veterinary Medicine, Zagreb, Croatia

[4] Department of Biology, University of Split Faculty of Science, Split, Croatia

[5] Department of Teacher Education, University of Split Faculty of Philosophy, Split, Croatia

[6] Department of Anatomy, Histology and Embryology, Laboratory for Early Human Development, University of Split School of Medicine, Šoltanska 2, 21000 Split, Croatia

Introduction

Diabetic nephropathy (DN) occurs as one of the most serious and frequent complications of both type 1 and 2 diabetes mellitus (DM) and is a leading cause of end-stage renal disease (Satirapoj 2013; Mora-Fernandez et al. 2014). Early structural and functional changes that influence development and progression of DN include kidney hypertrophy and glomerular hyperfiltration (Blantz and Singh 2014). A consequence is a damage of a glomerular filtration membrane, which was the primary focus of the DN research till recently. Nowadays, a research for a key therapeutic target in diabetic kidney disease was transferred to proximal tubules as a prime mover and the starting point in DN (Gilbert 2017; Vitlov Uljevic et al. 2018). Yet, not much attention was paid to the significance of the distal tubular cell (DTCs) damage in the early phase of DN, and its occurrence, pathophysiological changes and underlying mechanisms were still not explored.

Over recent years, there have been an increased interest in nutritional value and health benefits of long-chain polyunsaturated fatty acid (PUFA) consumption, due to the fact that numerous pathological conditions and changes in tissues are associated with PUFA alteration (Masek et al. 2014; Tosi et al. 2014; Takahashi et al. 2017). In addition to numerous protective effects that long-chain n−3 PUFA have shown on cardiovascular system (Bang et al. 1976; Simopoulos 1997; Horrocks and Yeo 1999; Yokoyama et al. 2007; Shoji et al. 2013), renoprotective effects of n−3 PUFA have also been shown in epidemiological studies of diabetic patients with type 2 and type 1 diabetes (Hamazaki et al. 1990; Shimizu et al. 1995; Mollsten et al. 2001), as well as in experimental models of DM (Barcelli et al. 1990; Fujikawa et al. 1994). Beneficial effects that n−3 PUFA exert in the kidney include prevention of albuminuria, glomerulosclerosis, tubulointerstitial fibrosis and inflammation associated with long-term diabetes (Garman et al. 2009). It is well-known that the position of the double bond in PUFA determines its effects on inflammation. In general, mediators formed from n−3 PUFA have anti-inflammatory effects; while those formed from n−6 PUFA are proinflammatory (Schmitz and Ecker 2008). An optimal dietary intake of the n−6/n−3 ratio is considered to be 1–4/1. As a result of the increased consumption of linoleic acid (LA)-rich vegetable oils in the modern Western diet, this ratio is estimated to be of 10:1 to 20:1 (Patterson et al. 2012). The effects of different dietary n−6/n−3 PUFA ratios are not fully explored, especially in conditions of DN.

Recently, we found changes in renal special AT-rich sequence-binding protein-1 (SATB1) expression during long-term DM1, which pointed out its possible role in the pathophysiology of DN (Delic Jukic et al. 2018). The role of SATB1, a tissue-specific nuclear matrix-binding protein, is widely explored in different types of cancer. In opposite to its high expression in tumours, expression of SATB1 was found to be low in healthy cells (Alvarez et al. 2000; Zhang et al. 2015). There is no much data about the role of SATB1 in other pathologies, but findings in damaged diabetic kidneys pointed out its important role in the pathophysiology of DN.

Vascular endothelial growth factor (VEGF) is an important factor in the pathophysiology of diabetic renal damage and pathogenic link between hyperglycaemia and early renal dysfunction. An increased renal VEGF expression was found in different experimental diabetic models (Ferrara 1999; Majumder and Advani 2016). In our previous work (Vitlov Uljevic et al. 2018) in a DM type 2 model, during prolonged hyperglycaemia, we found dynamic redistribution of VEGF in proximal tubular cells with VEGF present in vesicular apparatus of normal rat kidney and its translocation to apical membrane of PTC in a sucrose damaged renal tissue. Those data gave us a novel insight into the renal VEGF trafficking and initiated our new research which examined the effect of diet with different n−6/n−3 PUFA ratios in diabetic rats on VEGF endocytosis system.

The aim of this study was to explore the influence of streptozotocin-caused DM1 and potential protective/deleterious effects of different n−6/n−3 ratios on renal phospholipid composition and pathological changes caused by DM1. The accent of the research was on tubular damage, in particular, on damage of distal tubules, whose role in the pathophysiology of DN we find greatly underestimated. We also followed the expression pattern of SATB1, as possible novel marker for a distal tubular damage, as well as the VEGF expression pattern, which might be a potential marker for damage of the endocytotic vesicular system in PTCs.

Material and methods

Ethics

All experimental protocols were approved by the National Ethics Committee (EP 13/2015) and Veterinary Directorate, Ministry of Agriculture, Republic of Croatia, and conducted according to the Croatian Animal Welfare Act.

Experimental design

A total of 25 male Wistar rats were raised in standard polycarbonate cage under controlled environmental conditions (temperature at 22 ± 1 °C with a 12 h light/dark cycle). Different ratios of n−6/n−3 in the diet were accomplished by adjusting a standard laboratory chow (containing 20% crude protein, 5% crude fat and 5% crude fibre) using different oil blends, consisting of sunflower, fish and linseed oil, as was published in detail previously (Starcevic et al. 2018). Food and water were given ad libitum. The rats were randomly divided into 4 groups that received different n−6/n−3 ratios. Control group (C) received food with 0.5% of linseed oil and 2% of sunflower oil with n−6/n−3 ratio of 7. Second group (STZ) had the same feeding protocol; diet of STZ + N6 group contained 2.5% sunflower oil with n−6/n−3 ratio 60, while diet for STZ + DHA group contained 2.5% of fish oil, n−6/n−3 ratio of 1 with 16% eicosapentaenoic acid (EPA) and 19% docosahexaenoic acid (DHA) added. In order to induce diabetes, two weeks after beginning of the adjustment to the diet, all the groups except C were injected intraperitoneally with 55 mg/kg body weight of streptozotocin dissolved in citrate buffer (pH 4.5) after overnight fasting. Pure citrate buffer solution was given to the C group, as described previously (Vuica et al. 2015). Electronic balance was used to measure weight while glucose concentration in plasma was measured using a glucometer (Accu-Check Go). Rats were considered diabetic if the concentration of blood glucose was > 16.5 mmol/L.

Sample collection

Thirty (30) days after the streptozotocin/citrate buffer injection, the rats were sacrificed by exsanguination in deep anaesthesia (Narketan 80 mg/kg and Xylapan 12 mg/kg; Vétoquinol, Bern, Switzerland). Blood samples for malondialdehyde (MDA) measurement were taken directly from the heart, before exsanguinations, and collected in the presence of EDTA. Samples were centrifuged at 1500 ×*g* for 5 min, and plasma was separated and immediately frozen at − 80 °C. Kidneys were extracted and immediately frozen for protein extraction and fatty acid analyses or stored in buffered 4% paraformaldehyde for histological analyses.

Oxidative status measurement

Plasma MDA content was measured by HPLC method as MDA-TBARS (thiobarbituric acid-reacting substances), as described previously (Starcevic et al. 2018). Twenty microlitre aliquots were injected onto a Shimadzu LC-2010HT with an Inert-Sustain C18 column (4.6 × 150 mm, 5 μm particle size; GL Sciences, Tokyo, Japan), and the standard curve was prepared by using 1,1,3,3-tetraethoxypropane.

Lipid extraction and quantification of fatty acid composition

Total lipids (TL) from the kidney tissue were extracted according to Folch et al. (1957) with chloroform/methanol (2:1, *v*/*v*). As an antioxidant, butylated hydroxytoluene (BHT, Sigma-Aldrich, St. Louis, MO) was used (30 mg/100 ml). Solid-phase extraction on a 500 mg aminopropyl-bonded silica cartridge (Supelclean, Supelco, Bellefonte, PA, USA) was used to separate neutral lipids (NL) and total phospholipids (PL), using chloroform/isopropanol (2:1, *v*/*v*) for neutral lipids followed by methanol for phospholipids. Separated phospholipids were dried under N_2, redissolved in 200 μl of chloroform–methanol (2:1, *v*/*v*) with added BHT and stored at − 80 °C.

Fatty acids from PL were transmethylated using BF_3 in methanol at 64 °C for 3 h, extracted in n-hexane and transferred into vials containing anhydrous Na_2SO_4.

GC–MS (QP2010 Ultra; Shimadzu, Kyoto, Japan) equipped with capillary column BPX70 (0.25 mm internal diameter, 0.25 μm film thickness, 30 m length; SGE, Austin, TX, USA) was used for fatty acid methyl ester quantification. Analytical conditions were set as already published previously (Masek et al. 2017; Starcevic et al. 2018). For an internal standard, non-adecanoic fatty acid (C19:0) was used. The results were expressed as mole percentage of total fatty acids.

Protein extraction and Western blot analyses

The kidney tissue was homogenized in lysis buffer (RIPA lysis buffer, EMD Millipore, Billerica, MA, USA) with protease inhibitors (SIGMAFAST™ Protease Inhibitor Tablets, Sigma-Aldrich, Germany). Lysates were centrifuged for 10 min at 15,000 ×*g* (at 4 °C), and the supernatants were transferred to clear tubes. The protein concentration was measured by BCA assay (Sigma-Aldrich, Taufkirchen, Germany); bovine serum albumin was used as the standard. Forty microgrammes of total proteins was denatured by boiling (5 min) in Laemmli SDS loading buffer. They were run on 10% SDS polyacrylamide gel electrophoresis, and the proteins were electrotransferred to a nitrocellulose membrane. The membranes were blocked in blocking buffer (1% non-fat milk and 0.5% I-block protein-based blocking reagent) (Applied Biosystems) dissolved in Tris-buffered saline with 0.5% (*v*/*v*) Tween (TBST) for 1 h at room temperature. Incubation at 4 °C with different primary antibodies followed. Rabbit anti-VEGF antibodies (ab46154; Abcam, Cambridge, UK) and rabbit anti-NF-kB p65 antibody (ab7970; both diluted at 1:250) were used. The membranes were washed for three times with TBST buffer and incubated for 1 h at room temperature with horse radish peroxidase-conjugated goat anti-rabbit secondary antibodies (sc-2004; Santa Cruz Biotechnology; diluted at 1:2000). Detection was performed by chemiluminescence (Odyssey Fc, LI-COR, Bad Homburg, Germany). The expression levels of proteins were quantified relative to β-actin chemiluminescence as loading control (sc-130657; Santa Cruz Biotechnology; diluted at 1:250) by using ImageJ software (National Institutes of Health, Bethesda, MD, USA).

Kidney histology and immunohistochemistry

After washing in phosphate buffer (PBS, pH 7.2), tissues were dehydrated in a series of ethanol solutions and embedded in paraffin wax, as previously described (Vuica et al. 2015). Histological sections of 5 μm were made using the microtome and were placed on glass slides. After deparaffinization, tissues were rehydrated with ethanol and water and briefly rinsed with distilled water, and histological or immunohistochemical staining was performed. Standard histological Mallory Trichrome and PAS staining were performed as previously described (Agnic et al. 2013; Vitlov Uljevic et al. 2018).

Alternatively to paraffin embedding, renal slices ($n = 5$ per experimental group) were washed in PBS, cryoprotected in 30% sucrose and frozen in OCT medium (OCT, Tissue Tek, Tokyo, Japan), by using isopentane pre-cooled in liquid nitrogen. Five micrometre-thick sections were made by using cryotome (Thermo Shandon, Pittsburgh, PA, USA) and mounted on Histobond+ glass slides. After washing in PBS, the slides were stained in Oil Red solution (Oil Red O, C.I.

26125, BioGnost d.o.o., Zagreb, Croatia) for 2 min, counterstained in haematoxylin for 2 min, washed and cover-slipped.

Immunohistochemistry

After deparaffinization, sections were heated for 12 min in citrate buffer (pH 6.0), cooled down and washed in PBS. Sections were then incubated overnight in the following primary antibodies: rabbit anti-VEGF antibodies (anti-VEGF A antibody; ab46154; Abcam, Cambridge, UK; diluted at 1:200); rabbit anti-NF-kB p65 antibody (ab7970; diluted at 1:1000); and goat anti SATB1 (sc-5990, Santa Cruz Biotechnology Inc., Santa Cruz, CA, USA; diluted at 1:100). After washing in PBS, appropriate secondary antibody Rhodamine Red™ conjugated donkey anti-rabbit (711-295-152) diluted at 1:300, Rhodamine Red™ conjugated donkey anti-goat (1:400; 705-295-003; both from Jackson ImmunoResearch Laboratories, Inc., Baltimore, PA, USA) or donkey anti-mouse AlexaFluor 488 conjugated antibodies (1:400; ab150073; Abcam, Cambridge, UK) was applied for 1 h to perform the detection. The sections were washed in PBS, and nuclei were stained with DAPI. The slides were then air-dried and cover-slipped (Immu-Mount, Shandon, Pittsburgh, PA, USA).

Preparation of kidney tissues for electron microscopy

Tissues previously washed in PBS were cut on the vibratome. Twenty micrometre-thick sections were made. Sections were permeabilized in 50% ethanol, washed in PBS and incubated at + 4 °C for 48 h in primary VEGF A antibody (1:200). After incubation, the sections were washed and incubated overnight in secondary goat anti-rabbit gold conjugated antibodies (13064; 2 nm; British Biocell International, UK; 1:1000 dilution). Post-fixation in 1% osmium tetroxide for 1 h and dehydration in ascending series of acetone were made. Tissues were then embedded in DURCUPAN resin. The ultrathin sections (0.05 μm thick) were made and contrasted with 1% uranyl acetate and lead citrate. Ultrathin sections were then observed by a transmission electron microscope (JEM JEOL 1400, Japan).

Data acquisition and analysis

Prepared sections were viewed and photographed using a microscope (BX61, Olympus, Tokyo, Japan) and captured using a cooled digital camera (DP71, Olympus, Tokyo, Japan). ImageJ Software was used for further analyses.

For blinded PAS scoring and PAS analysis, the whole cortical section areas of the kidneys were captured under 100× magnification. Blinded PAS scoring of glomeruli was made according to the modified method from Yabuki et al. (2006). Between 62 and 123 glomeruli were analysed (all the glomeruli present per section), as described previously (Vitlov Uljevic et al. 2018). Eight-bit thresholded (default thresholding method) figures were analysed blinded and semi-automatically by using ImageJ. By using free-hand selection tool, each glomerulus was manually outlined, and the PAS+ percentage area was measured. Glomeruli with < 20% of the PAS+ area were scored as 0; 1 = 20.00–39.99%; 2 = 40.00–59.99%; 3 = 60.00–79.99%; and 4 = 80.00–100.00%. The score was calculated for each animal by using the following formula: {(0 × no. of 0 / total no.) + (1 × no. of 1 / total no.) + (2 × no. of 2 / total no) + (3 × no of 3 / total no) + (4 × no of 4 / total no)} × 100. The number of total and glomeruli with thickened Bowman's capsule (BC; more than a half of the BC perimeter positively stained) was counted, and the percentage of glomeruli with thickened BC was calculated.

For analysis of DTC damage, 10–12 figures of slides stained by Mallory trichrome staining were captured under 200× magnification. The number of total distal tubules and those with vacuolated DTCs was counted, and the percentage of vacuolated distal tubules profiles was calculated.

Whole cortical section area of Oil Red-stained samples was captured under 400× magnification (non-overlapping visual fields were made) and analysed for existence, density and size of red-stained lipid droplets. The number of negative, weakly positive (few droplets) and strongly positive proximal tubules was counted, and the percentages of total, weakly and strongly lipid positive PT were calculated.

The number of total and SATB1-immunoreactive DTCs was counted by using ImageJ cell counter option on 10 visual fields, captured at 400× magnification, and the percentage of SATB1-immunoreactive DTCs was calculated. At the same time, a number of SATB1-immunoreactive glomerular cells were counted as well as their number expressed per analysed glomeruli.

For VEGF analysis, the number of total and granular pattern VEGF-positive proximal tubules was counted on six visual fields (400× magnification), and the percentage was calculated.

Statistical analyses

GraphPad Prism 5 Software (McIntosh, CA, USA) was used for statistical analyses. N was 5–6 per group for each measurement, with exception of fatty acid composition analysis (N = 4–5) and Western blot analysis (N = 3–4). One-way Analysis of Variance (ANOVA) was used with Tukey–Kramer multiple comparison test to determine significant differences among individual groups, in case of normal data distribution, according to Kolmogorov–Smirnov test. In opposite case (Kolmogorov–Smirnov test at $p < 0.05$), non-parametric Kruskal–Wallis and Dunn's multiple comparison test were used. Statistical significance was set up at $p < 0.05$.

Results

Blood glucose and plasma oxidative status

Mean blood glucose (mmol/L) of all three diabetic groups of rats was significantly higher in comparison to the control group (Fig. 1a; $p < 0.001$). Different diet composition did not result in change in blood glucose in STZ + DHA or STZ + N6, when compared to the normally fed diabetic rats (STZ group; $p > 0.05$). Plasma level of the MDA was significantly increased in all three diabetic groups, in comparison to the control group (Fig. 1b; $p < 0.001$). In addition, the level of the MDA was higher in STZ + DHA, when compared to STZ ($p < 0.01$) and STZ + N6 groups ($p < 0.001$).

Fatty acid composition of the renal phospholipids

Details of fatty acid composition of renal phospholipids are presented in Table 1. When summarized, DM1 resulted in significant decrease in saturated fatty acid (SFA; $p < 0.001$) content (Fig. 1c). That decrease was also observable in STZ + N6 and STZ + DHA experimental groups ($p < 0.001$ in comparison to C). Moreover, DHA supplementation caused additional decrease in SFA content in phospholipids, compared to the STZ group. In opposite, molar % of monounsaturated fatty acids (MUFA) increased in all three diabetic groups, in comparison to the control ($p < 0.001$; Fig. 1d). However, n−6 PUFA supplementation resulted in the decrease of MUFA in phospholipids of STZ + N6, in comparison to the STZ group ($p < 0.05$). On the other hand, molar % of MUFA in phospholipids of STZ + DHA

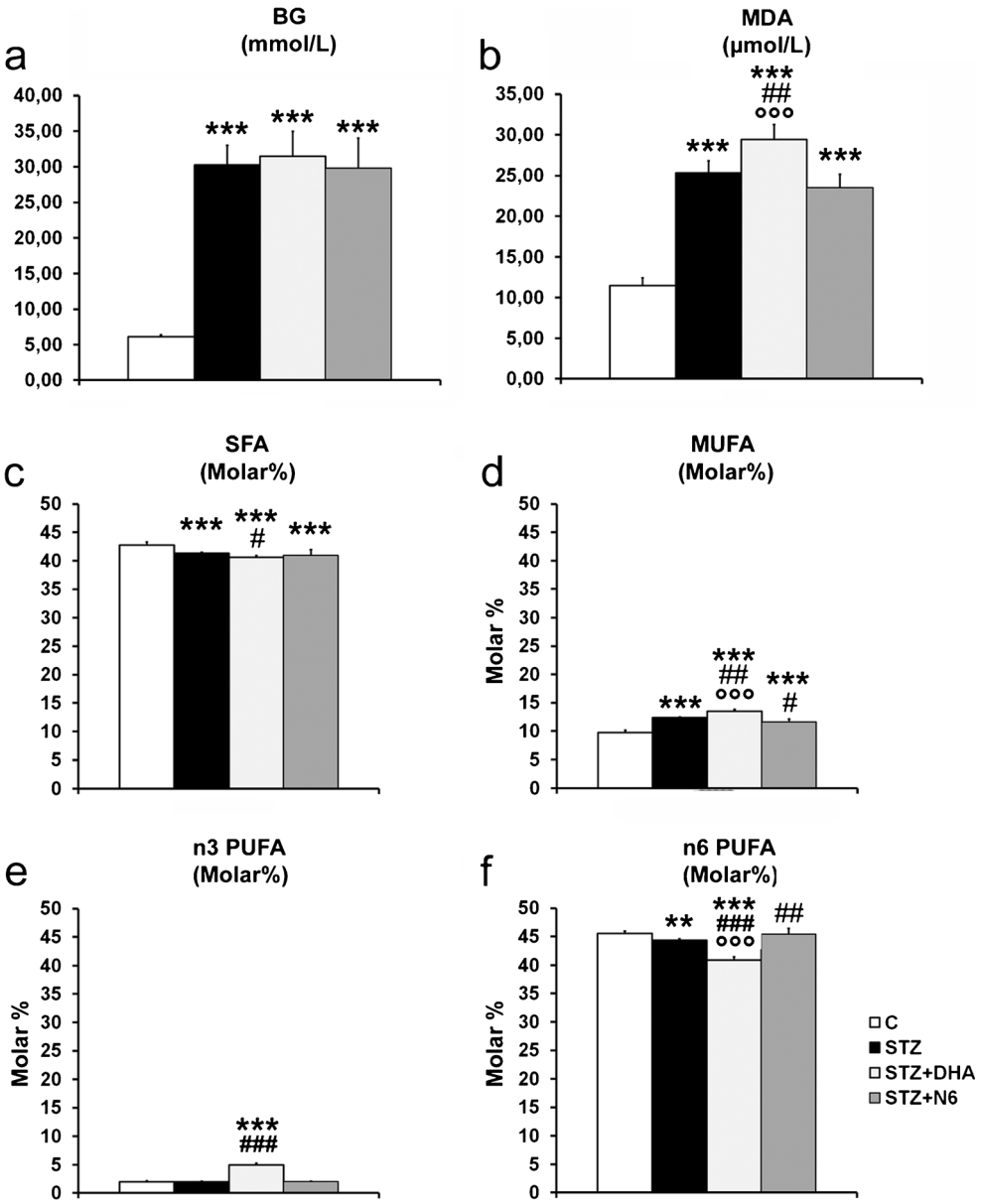

Fig. 1 Plasma glucose and malondialdehyde concentrations and fatty acid composition of the renal phospholipids. (**a**) Plasma glucose levels at the end of experiment in 4 experimental subgroups of animals. (**b**) Levels of plasma malondialdehyde (MDA). (**c**–**f**) Molar fraction of different fatty acids in renal phospholipids of 4 experimental subgroups of rats. (**c**) Molar % of saturated fatty acid (SFA); (**d**) monounsaturated fatty acids (MUFA); (**e**) omega 3 (n−3) and (**f**) omega 6 (n−6) PUFAs. C, control group; STZ, DM1 group; STZ + DHA, DM1 group fed with n−6/n−3 ratio of 0.05 (16% EPA and 19% DHA); STZ + N6, DM1 group with n−6/n−3 ratio of 60. $^{**}p < 0.01$; $^{***}p < 0.001$ vs. C; $\#p < 0.05$, $\#\#p < 0.01$; $\#\#\#p < 0.001$ vs. STZ; $^{\circ\circ\circ}p < 0.001$ vs N6

was the highest, being higher compared to both STZ and STZ + N6 groups ($p < 0.01$ and $p < 0.001$, respectively).

As expected, content of n−3 PUFA was the highest in the STZ + DHA group, being significantly higher in comparison to both control and STZ groups ($p < 0.001$). However, n−3 PUFA content was not influenced by DM1, alone or in combination with n−6 treatment (Fig. 1e). In opposite to n−3, content of n−6 PUFA was the lowest in the STZ + DHA group ($p < 0.001$, compared to C, STZ and STZ + N6). DM1 by itself caused significant decrease in n−6 PUFA phospholipid content, while in the STZ + N6 group, n−6 PUFA content was preserved on the level of the control group (Fig. 1f).

Influence of DM1 and PUFA supplementation on distal tubules of the rat kidney

Mallory trichrome staining

Histological sections of kidneys in control rats have shown normal structure of DTCs (Fig. 2a). Sections from kidneys in all three diabetic groups contained many vacuolated distal tubules, whose cell structure was completely destroyed (Fig. 2b–d). Analysis revealed significantly higher % of distal tubules with vacuolated cells in kidneys of all diabetic rats, but significantly lower percentage was present in DTCs of the STZ + DHA group (Fig. 2e). Oil Red staining did not show any sign of lipid accumulation in DTCs (Fig. 7). PAS staining denied glycogen accumulation in DTCs (Fig. 2f).

Ultrastructural analysis of distal tubular cells

Ultrastructural analysis of DTCs in diabetic groups of rats has shown shrinking of the nuclei, with condensation of the chromatin and almost complete loss of the cytoplasm (Fig. 3b–f). Mitochondria were damaged and along with the other organelle they were pushed down and concentrated exclusively in basolateral cellular compartment. Ultrastructural analysis confirmed that there was no lipid or glycogen accumulation in DTCs.

NF-kB expression

Additionally, we made NF-kB immunohistochemical staining in distal tubules of experimental rats. The strongest NF-kB immunofluorescence was observed in distal tubules (Fig. 4a–d). Western blot analysis revealed significant increase in the

Table 1 Fatty acid composition of the phospholipids in kidney

	Control (C)		STZ			STZ + DHA			STZ + N6			*P*
	M ± SD		M ± SD			M ± SD			M ± SD			ANOVA
C14:0	0.13	± 0.01	0.07	± 0.01	***	0.08	± 0.01	***	0.10	± 0.02	**#	< 0.0001
C16:0	21.52	± 0.18	21.57	± 0.10		21.31	± 0.62	°°	20.20	± 0.30	***###	0.0002
C16:1	0.23	± 0.05	0.04	± 0.01	***	0.21	± 0.03	°°°###	0.07	± 0.02	***	< 0.0001
C18:0	21.10	± 0.48	19.69	± 0.12	***	19.23	± 0.49	***°°°	20.67	± 0.21	##	< 0.0001
C18:1n−9	7.91	± 0.33	10.92	± 0.12	***	10.99	± 0.20	***°°	10.11	± 0.52	***#	< 0.0001
C18:1n−7	1.60	± 0.14	1.38	± 0.03	*	2.31	± 0.13	***###°°°	1.43	± 0.07		< 0.0001
C18:2n−6	10.75	± 0.75	12.34	± 0.14	*	16.15	± 0.81	***###	13.14	± 0.67	***	< 0.0001
C18:3n−3	0.03	± 0.02	0.06	± 0.01		0.00	± 0.00	*###°°°	0.13	± 0.02	***###	< 0.0001
C20:3n−6	0.47	± 0.08	0.62	± 0.02	*	0.60	± 0.05	*	0.61	± 0.07	*	0.0112
C20:4n−6	34.09	± 0.96	31.06	± 0.28	***	24.17	± 0.68	***###°°°	31.48	± 1.05	**	< 0.0001
C20:5n−3	0.22	± 0.07	0.03	± 0.02		1.28	± 0.22	***###°°°	0.11	± 0.04		< 0.0001
C22:4n−6	0.21	± 0.04	0.30	± 0.03	*	0.02	± 0.04	***###°°°	0.18	± 0.04	###	< 0.0001
C22:5n−3	0.15	± 0.03	0.15	± 0.01		0.23	± 0.04	*#°	0.16	± 0.04		0.0067
C22:6n−3	1.60	± 0.05	1.77	± 0.05		3.43	± 0.23	***###°°°	1.62	± 0.11		< 0.0001

*$p < 0.05$
**$p < 0.01$
***$p < 0.001$ vs. C
#$p < 0.05$
##$p < 0.01$
###$p < 0.001$ vs. STZ
°$p < 0.05$
°°$p < 0.01$
°°°$p < 0.001$ vs. N6

STZ + DHA subgroup of rats compared to the control group ($p < 0.05$; Fig. 4e). There was no statistical significance between the control and the STZ group and the STZ + N6 group.

SATB1 expression

We applied immunohistochemistry to analyse the SATB1 expression in cortical sections of the kidneys of the experimental rats. We found very weak SATB1 expression in proximal tubule. In opposite to the expression in the PTCs, very strong SATB1 immunoflourescence was found in DTCs of the diabetic rats (Fig. 5). However, the SATB1 immunoflourescence was found very rarely in DTCs of the control, non-diabetic rats. We analysed the total number of DTCs and the number of cells with positive SATB1 expression in distal tubules in all subgroups of animals. An increased percentage of SATB1-immunoreactive DTCs was found in STZ + DHA and STZ + N6 groups, in comparison to the control group ($p < 0.01$). We also analysed a number of SATB1-positive cells per glomerulus, but we did not find any statistically significant difference between groups (data not shown).

PAS staining

PAS staining in glomeruli revealed higher mesangial expansion in DM1 groups of rats (Fig. 6a–c). Analysis has shown prominent accumulation of PAS staining in Bowman's capsule (BC) of the rats in the STZ + N6 subgroup (Fig. 6d).

Influence of DM1 and PUFA supplementation on proximal tubules of the rat kidney

Ectopic lipid accumulation in proximal tubules of diabetic rats

No signs of lipid accumulation were found in the kidney sections from the control rats. Oil Red staining revealed that DM1 caused pronounced accumulation of neutral lipids in PTCs (Fig. 7a–a''' and b). Lipid accumulation was not found in

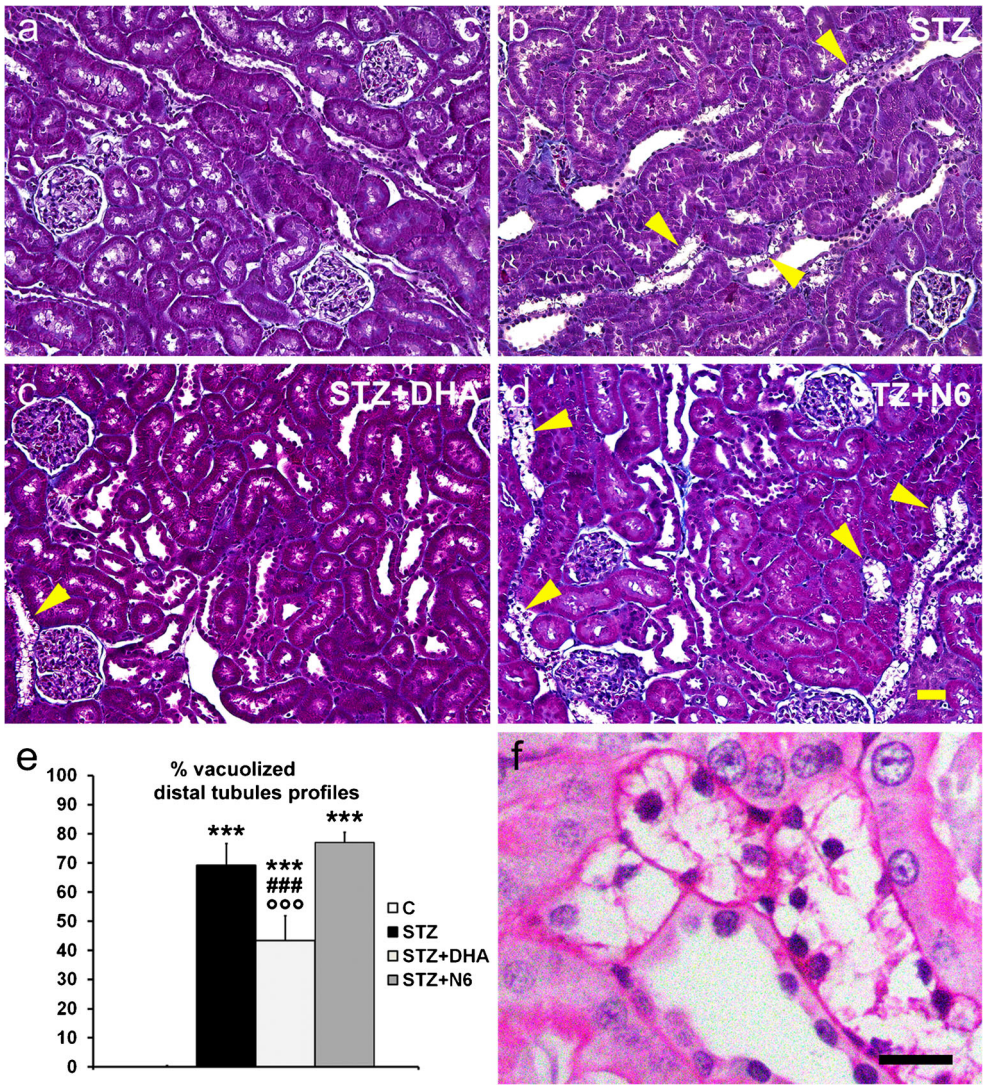

Fig. 2 Mallory trichrome staining in the kidney of the experimental rats. Normal structure of DTCs in the histological sections of kidney, in the control group of rats (**a**). Destroyed cellular structure with vacuolated distal tubules is evident in all subgroups of experimental animals with DM1 (STZ, STZ + DHA, STZ + N6; **b**–**d**). Quantification of the percentage of vacuolated distal tubules (**e**). Representative microphotography of PAS staining shows destroyed, vacuolated distal tubules (next to the preserved tubule) and reveals a lack of any glycogen accumulation (**f**). C, control group; STZ, DM1 group; STZ + DHA, DM1 group fed with n−6/n−3 ratio of 0.05 (16% EPA and 19% DHA); STZ + N6, DM1 group with n−6/n−3 ratio of 60. *$p < 0.05$, ***$p < 0.001$ vs. C. Scale bar on **d** = 40 μm (refers to **a**–**d**); scale bar on **f** = 20 μm

DTCs or in glomeruli. Sections from the STZ-N6 group had the highest percentage of strongly and total (strong + weak) Oil Red-positive proximal tubules (Fig. 7b). TEM confirmed the existence of the LDs in PTC cytoplasm, which was the most pronounced in the STZ + N6 group. LDs found in PTCs were concentrated in the basolateral cellular compartment; they were larger in diameter than endocytotic vesicles and they had very strong electron density (Fig. 7c; Fig. 9a–d).

Influence of DM1 and PUFA supplementation on VEGF expression in PTCs

Kidneys of the control group of rats showed significantly higher number of proximal tubules with VEGF-immunoreactive granules in cytoplasm in comparison with all the other groups of animals ($p < 0.001$; Fig. 8e). In all the groups which were given streptozotocin, very intense VEGF immunofluorescence is still observed, but it is more diffuse and not concentrated in the form of highly expressed granular pattern as it was in the control group of rats. The smallest number of tubules with preserved granular pattern was found in the STZ + N6 group ($p < 0.05$). However, despite the remarkable expression pattern change, Western blot analysis did not show significant differences between groups in VEGF protein expression ($p > 0.05$; Fig. 8f).

TEM microphotographs of the proximal tubules stained for VEGF

TEM additionally confirmed results of the light microscopy, concerning ectopic lipid accumulation and VEGF expression

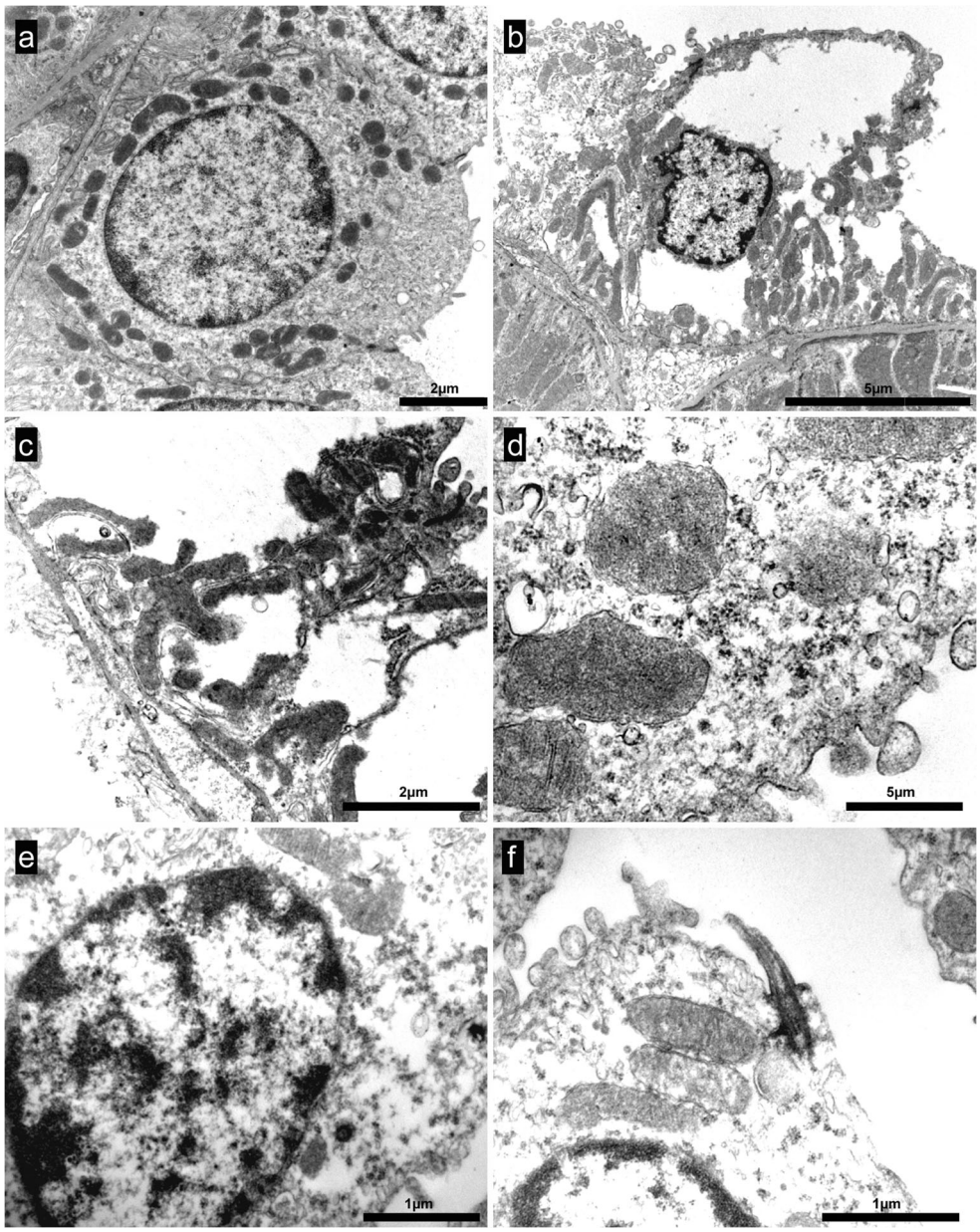

Fig. 3 Transmission electron microscopy (TEM) microphotographs of the distal tubules. Representative TEM microphotographs of the distal tubules (**a**–**f**). (**a**) Preserved distal tubular cell (DTC). Ultrastructural analysis of DTCs of diabetic rat revealed a loss of the cytoplasm (**b**–**d**), shrinking of the nucleus (**b**) and condensation of the chromatin (**b** and **e**). Mitochondria and the other organelle are damaged (**c** and **d**) and pushed down in basolateral cellular compartment (**b** and **c**). (**f**) Apical part of the damaged DTC, with cilia. There is no lipid or glycogen accumulation (**b**–**f**)

pattern (Fig. 9). PTCs from the C group had many VEGF-immunoreactive vesicles in the cytoplasm, while in the kidneys of the rats from the STZ group, VEGF-immunoreactive vesicles were still present but lesser in number. Their cytoplasm contained many LDs, which were larger in comparison to the vesicles and had very high electron density. Cytoplasm of the PTCs of rats from the STZ + DHA group also contained LDs, while VEGF-immunoreactive vesicles are very rare. In the cytoplasm of the PTCs of the STZ + N6 rats, many large LDs were found along with rare VEGF-immunoreactive vesicles. High-power magnification has shown that VEGF immunoreactivity was condensed on the superficial parts of the vesicles and their membrane. Strong VEGF immunoreactivity was present occasionally at the base of the brush border of the PTCs' apical membrane. Damaged mitochondria and deformed endocytotic vesicles were observed in the PTC of diabetic rats. Strong VEGF immunoreactivity was also present in pedicles of the podocytes in diabetic rats, confirming continuous renal VEGF production (data not shown).

Discussion

The results of our study have proved substantial change in renal phospholipid fatty acid composition in streptozotocin-induced DM1 rat model which was strongly influenced by dietary PUFA composition. Excess of n−6 PUFA in diet of diabetic rats prevented decrease of n−6 in phospholipids caused by DM1, but it resulted in lower level of phospholipid monounsaturated fatty acids (MUFA). On the other hand, DHA/EPA supplementation resulted in increase of n−3 PUFA and MUFA phospholipid renal content, in the expense of decrease in n−6 PUFA. Our data are in agreement with results of research conducted by Di Stasi and collaborators, who proved that diet supplementation with different amounts of EPA and DHA can rapidly change the composition of fatty acids in blood cell membranes and presumably in other tissues (Di Stasi et al. 2004).

Decrease in saturated fatty acids (SFA) and simultaneous increase in MUFA renal phospholipid content that we observed in DM1 could be explained by overexpression of stearoyl-CoA desaturase-1 (SCD-1), a key enzyme responsible for converting lipotoxic SFA to less lipotoxic MUFA, which can be an adaptive mechanism associated with metabolic disorders (Pinnamaneni et al. 2006; Paton and Ntambi 2010), in addition to the loss of lipogenic influence of insulin on fatty acid synthesis (Starcevic et al. 2018).

The highest content of n−3 PUFA, in particular EPA and DHA, in renal phospholipids of the STZ + DHA group reflected their higher availability from a diet. The lowest phospholipid content of n−6 PUFA in the STZ + DHA group probably resulted from n−3/n−6 competition (Holman et al. 1983).

The most prominent pathological change that we observed in kidneys of the STZ-DM1 rats was dramatic vacuolization of distal tubular cells (DTCs). We found similar changes in all our DM1 studies (unpublished data). However, it is

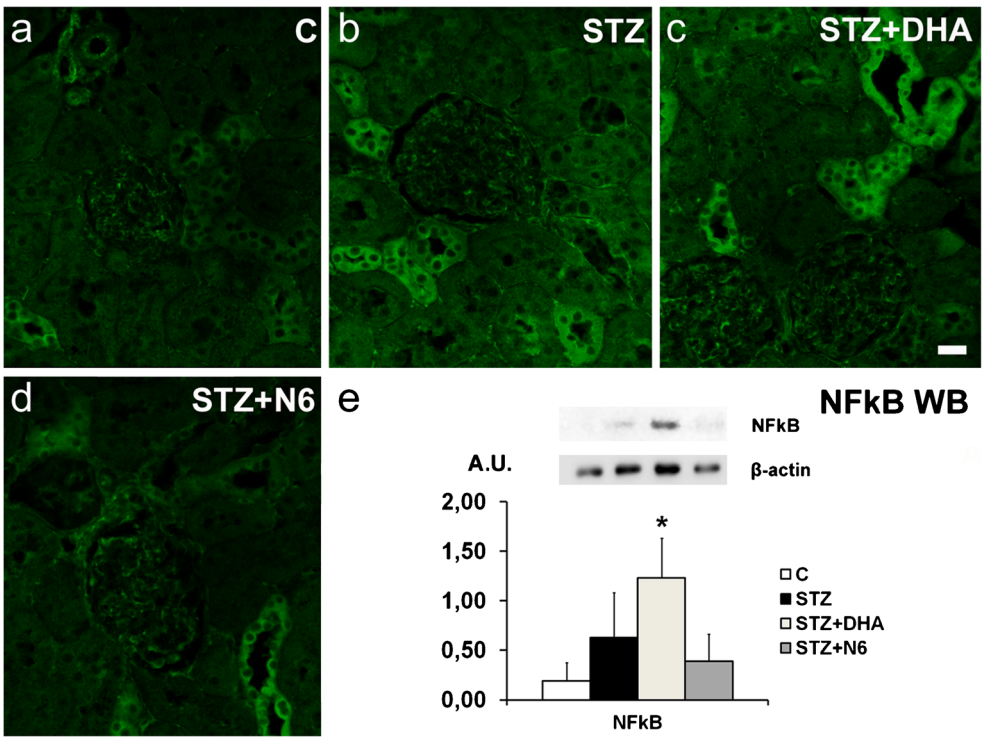

Fig. 4 NF-kB expression in kidneys of experimental rats. Representative microphotographs of renal NF-kB expression of experimental rats. The strongest NF-kB immunofluorescence was observed in distal tubules. (**a**) C, control group; (**b**) STZ, DM1 group; (**c**) STZ + DHA, DM1 group fed with n−6/n−3 ratio of 0.05 (16% EPA and 19% DHA); (**d**) STZ + N6, DM1 group with n−6/n−3 ratio of 60. (**e**) Western blot (WB) quantification of NF-kB expression demonstrates statistically significant increase in STZ + DHA subgroup of rats compared to the C (*$p < 0.05$). Scale bar = 20 μm

noteworthy that in our model of long-term high-sucrose-provoked metabolic syndrome, we did not observe DTC vacuolization, despite substantial renal damage (Vitlov Uljevic et al. 2018). Taking into consideration lack of Oil Red and PAS staining in DTCs, we can exclude lipid or glycogen accumulation. These findings are confirmed by ultrastructural examination. We can assume that accumulation of water that we found in DTCs of DM1 rats might be a result of detrimental effect of the hyperglycaemia/and or insulin deprivation on membrane transport in the DTCs. However, results of our study revealed that DHA/EPA supplementation partially decreased detrimental influence of DM1 on DTCs. It was known that long-chain PUFAs inserted into membrane phospholipids serve as oxygenated PUFA precursors (Shapiro et al. 2010). Oxygenated PUFAs participate in the regulation of cellular and tissue function, which is mediated by altered activity of functional proteins from the cell membrane to the nucleus, as well as by modulation of the ion channels and transcription factors (Calder 2007; Simopoulos 2009). This could be an explanation for the protective effects of increased DHA/EPA renal phospholipid content on vacuolization of DTCs caused by DM1.

Additional explanation for the protective effects of n −3 supplementation could be, at least partially, increased expression of pro-survival inflammatory factor NF-kB Lawrence 2009), whose highest expression we found in kidneys of STZ-DHA group and was the most prominent in DTCs.

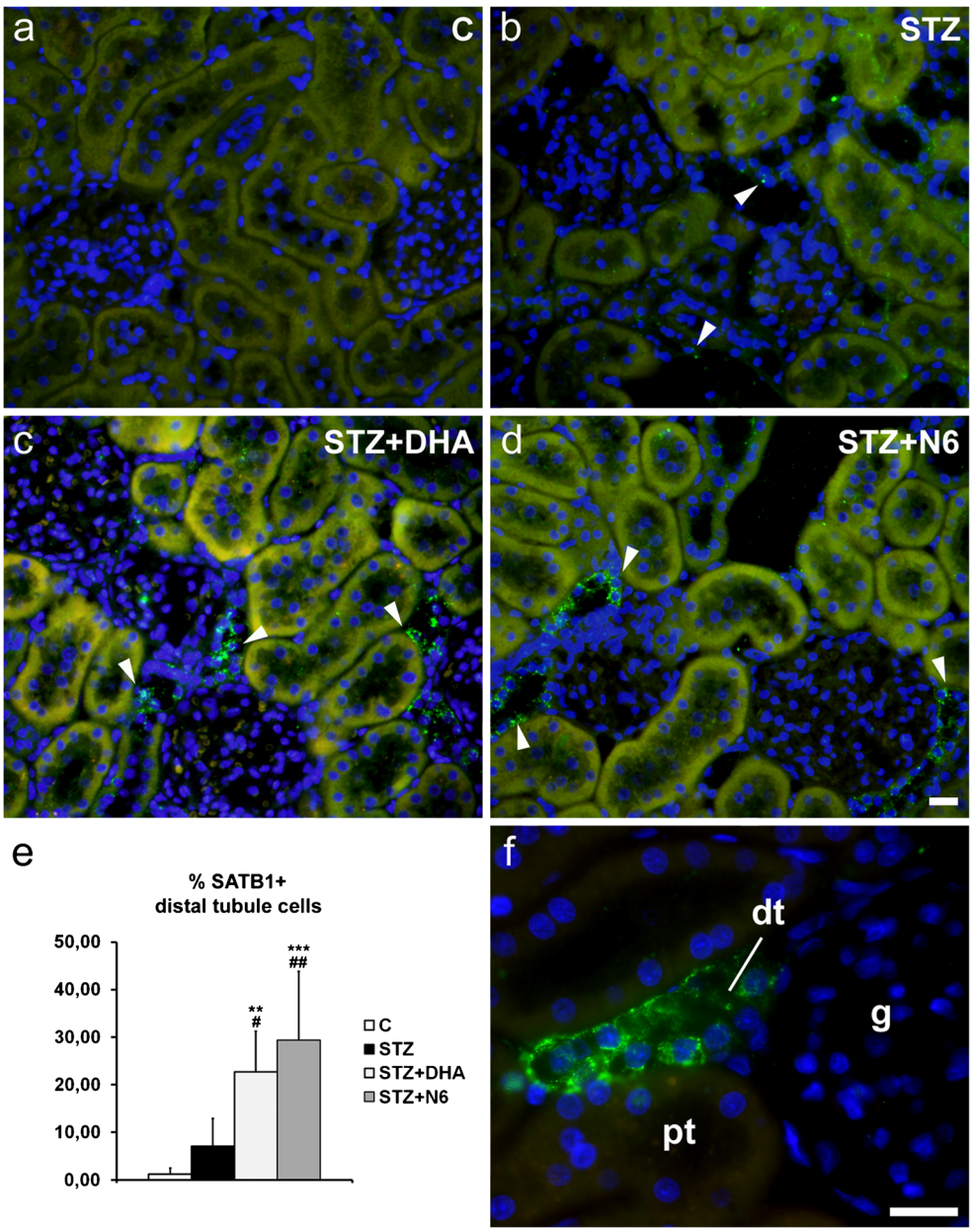

Fig. 5 SATB1 expression in kidneys of experimental rats. Representative microphotographs of renal SATB1 expression in experimental rats. Control group of animals (**a**), STZ group (**b**), STZ + DHA group (**c**) and STZ + N6 group (**d**). Arrowheads are showing SATB1-immunoreactive DTCs. Quantification of cells with positive SATB1 expression in total number of distal tubule cells revealed increased SATB1 expression in STZ + DHA and STZ + N6 groups compared with the control group ($p < 0.01$; **e**). Representative microphotography of SATB1 expression in distal tubule of STZ + N6 subgroup of experimental animals with highest expression (100× objective magnification; **f**). g, glomerulus; pt, proximal tubule; dt, distal tubule; scale bar on **d** = 20 μm (refers to **a**–**d**); scale bar on **f** = 20 μm

The DTC damage could also be related to the observed increased expression of SATB1. Namely, we found strong expression of SATB1 in damaged DTCs. Nevertheless, only kidneys from diabetic rats that were additionally supplemented by PUFA had significantly increased number of SATB1-immunoreactive DTCs. In our previous work (Delic Jukic et al. 2018), we found changes in expression of SATB1 in streptozotocin-induced DN which may point out to its role in

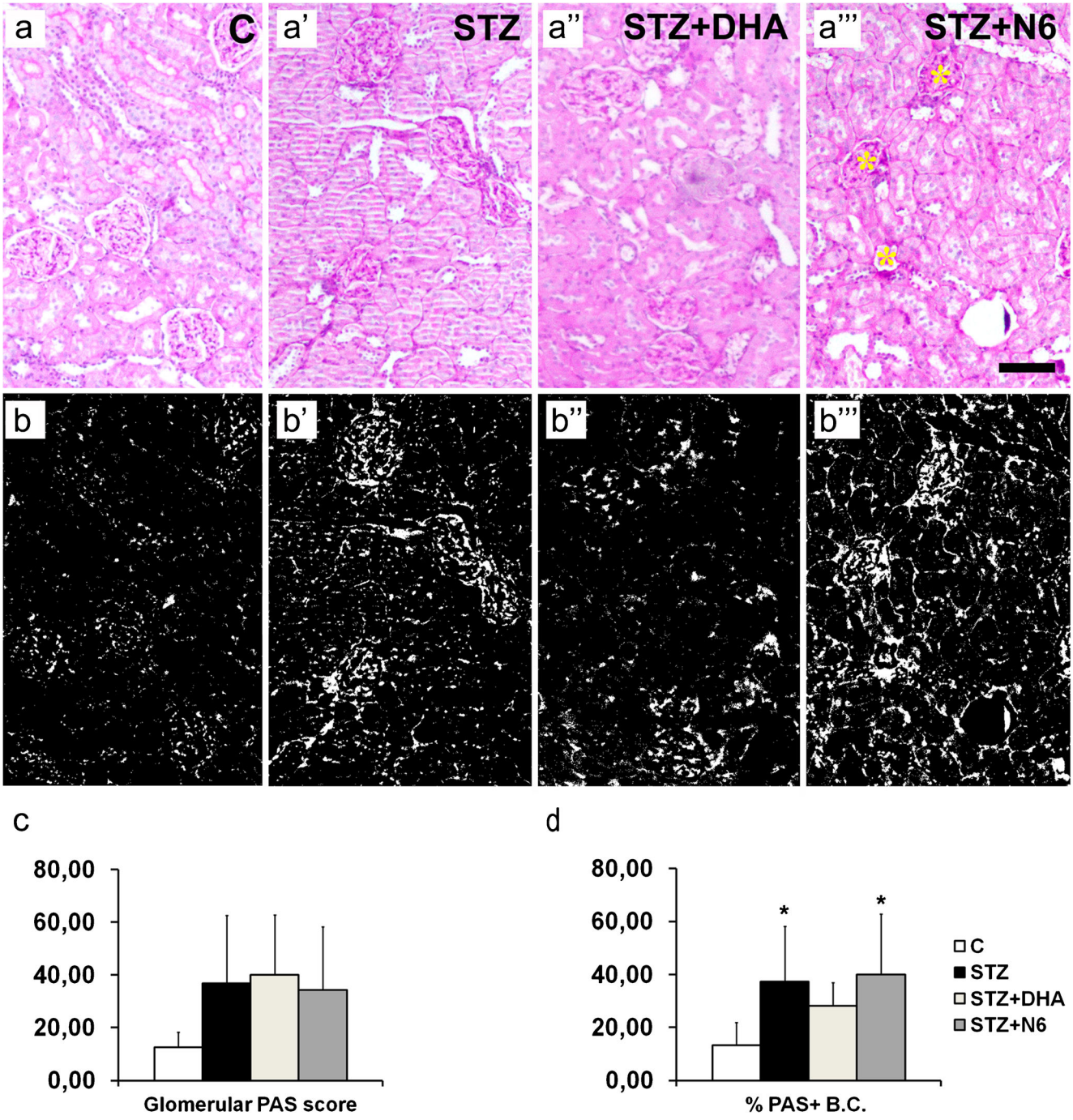

Fig. 6 PAS staining in the renal tissues of the experimental rats. (**a**–**a**''') Representative microphotographs of total area of PAS staining of experimental groups. (**b**–**b**''') The same microphotographs of total PAS area with subtracted background and thresholded surface of the intense pink staining. (**c**) Glomerular PAS score; (**d**) quantification of total PAS-stained accumulation area; (**e**) quantification of glomeruli with thickened Bowman's capsule (BC) showed prominent accumulation of PAS staining in BC of rats in the STZ + N6 subgroup. (**f**) Higher magnification representative microphotography of glomeruli with thickened Bowman's capsule (asterisk). C, control group (**a**, **b**); STZ, DM1 group (**a**', **b**'); STZ + DHA, DM1 group fed with n−6/n−3 ratio of 0.05 (16% EPA and 19% DHA; **a**'', **b**''); STZ + N6, DM1 group with n−6/n−3 ratio of 60 (**a**''', **b**'''). *$p < 0.05$ vs. C; °$p < 0.05$ vs. STZ + N6. Scale bar = 100 μm

the pathophysiology of DN. Here, we found the strongest expression of SATB1 in DTCs. In agreement with previous findings (Alvarez et al. 2000; Zhang et al. 2015), expression of SATB1 was very low in healthy DTCs which indicates its possible role in the pathophysiology of DTC damage. However, the role of SATB1 in damage/potential protection of DTCs during diabetic hyperglycaemia and its relation to PUFA supplementation deserve further clarification.

In studies of DN pathophysiology, the most attention was given to damage of the glomeruli. Nowadays, it is also recognised that tubular hypoxia plays an important role in the pathogenesis of chronic kidney disease and that the initial target for diabetic renal damage is proximal tubular cell (PTC) whose dysfunction causes the damage of glomerular filtration membrane (Gilbert 2017). However, less attention has been given to distal tubule damage, despite crucial roles of distal tubules in the regulation of acid–base balance and blood pressure. Drastic distal tubular damage, which we observed in more than one experiment using STZ-provoked DM1 rat models, points to the necessity of additional investigation of frequency, pathophysiological mechanisms and consequences of this component of DN pathology.

In order to reveal additional pathological changes, we also applied the PAS staining. Expected mesangial expansion in glomeruli of diabetic rats was not prominent and was variable. The most prominent significant change was thickening of the Bowman's capsule with accumulation of the PAS-positive material in glomeruli of diabetic rats treated with extra n−6

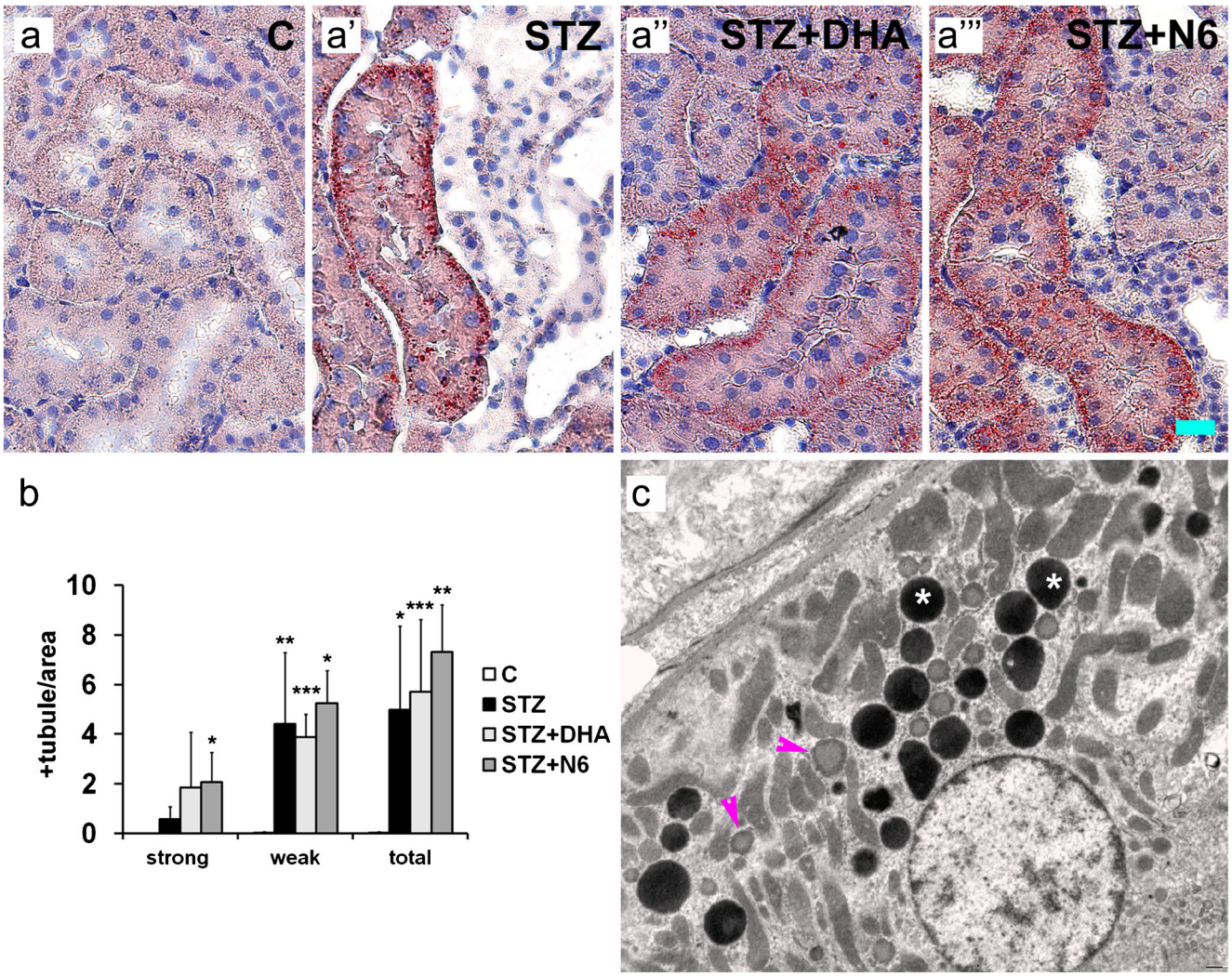

Fig. 7 Ectopic lipid accumulation in kidneys of the experimental rats. (**a**–**a**''') Representative microphotographs of Oil Red staining in proximal tubular cells (PTCs) in different subgroups of animals with no lipid accumulation in PTC of control rats and frequent appearance in PTCs of STZ, STZ + N6 and STZ + DHA subgroups. (**b**) Quantification of Oil Red-positive proximal tubules; (**c**) quantification of lipid droplet (LD) area fraction; (**d**) number of LD per area unit; (**e**) index of the LD size. (**f**) Representative TEM microphotographs of PTCs with evident lipid droplets (asterisk) in PTC cytoplasm, pronounced in the STZ + N6 group. (**g**) Higher magnification representative TEM microphotograph of PT with LD showing strong electron density (asterisk). C, control group (**a**); STZ, DM1 group (**a'**); STZ + DHA, DM1 group fed with n−6/n−3 ratio of 0.05 (16% EPA and 19% DHA; **a**''); STZ + N6, DM1 group with n−6/n−3 ratio of 60 (**a**'''). *$p < 0.05$; **$p < 0.01$; ***$p < 0.001$ vs. C. Scale bar on **a** = 20 μm

PUFA. Despite beneficial effect of n−3 PUFA supplementation on DTCs, we found the highest interstitial PAS accumulation in the STZ-DHA diabetic rats. Nevertheless, the highest MDA, lipid peroxidation indicator, has been found in the plasma of the same experimental group. This is not surprising, if we take into consideration that PUFAs are major substrates for lipid peroxidation (Yin et al. 2011). Increased intake of fish oils is associated with elevated susceptibility of membranes to oxidation (Ibrahim et al. 1999; Yilmaz et al. 2002). In erythrocytes of streptozotocin-induced diabetic rats, level of MDA was higher in the group of diabetic rats which were given fish oil (Yilmaz et al. 2002). Membranes rich in PUFAs are potentially vulnerable to oxidative damage, and the susceptibility of fatty acids to oxidation by reactive oxygen species increases with desaturation (Liu et al. 1997). DHA and EPA are rich with number of sites of desaturation (6 and 5), while n-6 omega fatty acids as linoleic and alpha-linoleic acid consist 2 or 3 desaturation positions. This clarifies the data obtained by our research in which the group supplemented in DHA/EPA had the highest level of plasma MDA.

DM1 caused pronounced accumulation of neutral lipids in proximal tubular cells (PTCs), which was present also in n−6 and DHA-treated diabetic groups. Lipid accumulation was restricted almost exclusively to PTCs and was not found in DTCs or in glomeruli. This lipid accumulation was the most prominent in kidneys from diabetic rats supplemented with n −6 fatty acids. In diabetic rats supplemented with DHA/EPA, PTC lipid accumulation was also evident, but it was variable and less prominent in comparison to the STZ

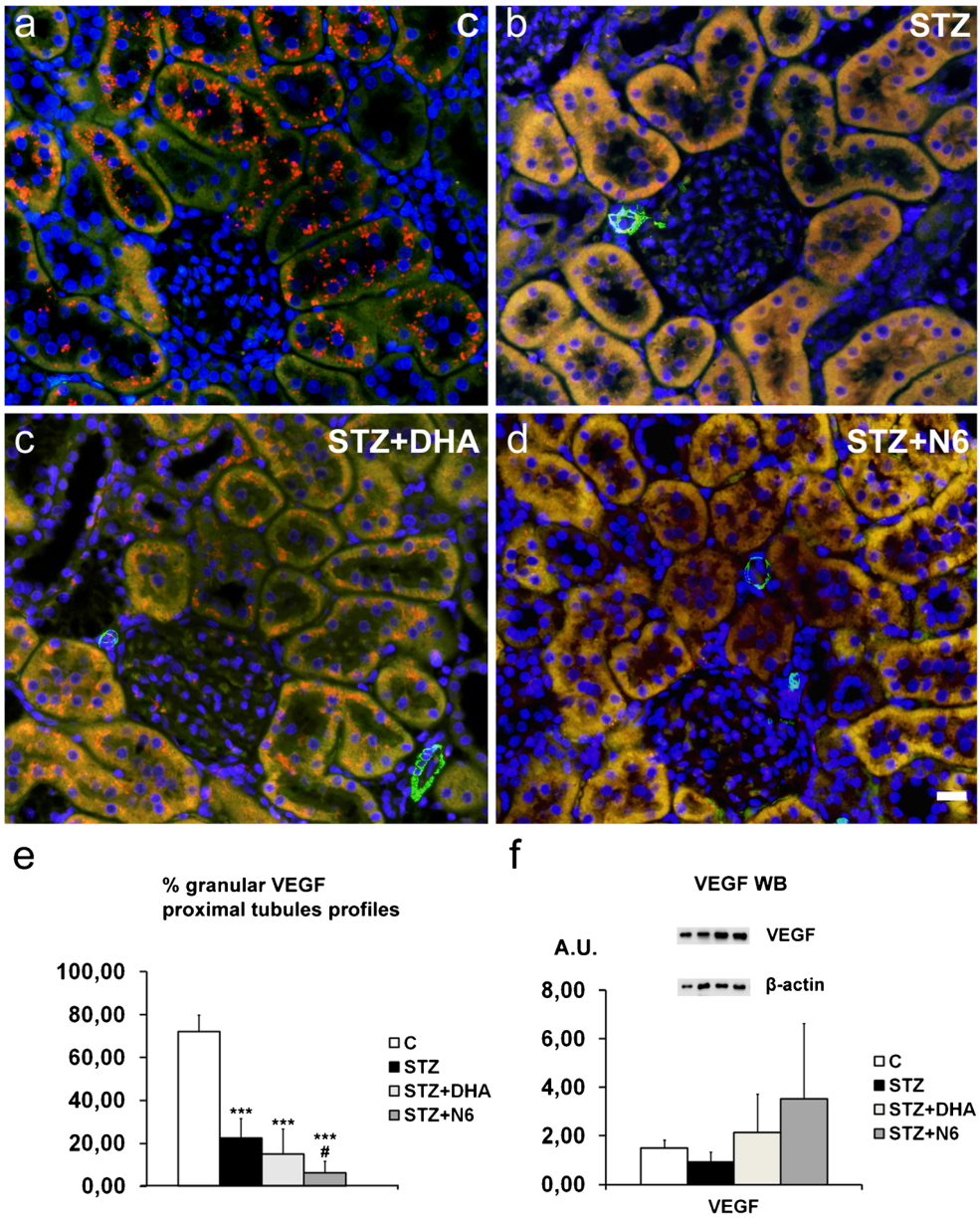

Fig. 8 Expression of VEGF in proximal tubules of experimental rats. (**a**) Representative microphotographs of VEGF expression (red) evident as strong granular pattern in PTCs of control group of animals. Sections were counter-stained for alpha smooth actin (green, in vessel wall), and nuclei were stained with DAPI (blue). (**b**–**d**) Representative microphotographs of DM1 animals with more diffused PT VEGF staining and very rare VEGF-immunoreactive granules in the cytoplasm. (**e**) Quantification revealed the smallest percentage of tubules with preserved granular VEGF pattern in all DM1 subgroups ($p < 0.001$). STZ + N6 group had a significantly smaller number of tubules with preserved granular pattern in comparison to the DM group ($p < 0.05$). (**f**) Despite the remarkable expression pattern change, Western blot (WB) analysis did not show significant differences between groups in VEGF protein content. C, control group; STZ, DM1 group; STZ + DHA, DM1 group fed with n−6/n −3 ratio of 0.05 (16% EPA and 19% DHA); STZ + N6, DM1 group with n−6/n−3 ratio of 60. ***$p < 0.001$ vs. C; #$p < 0.05$ vs. STZ. Scale bar = 20 μm

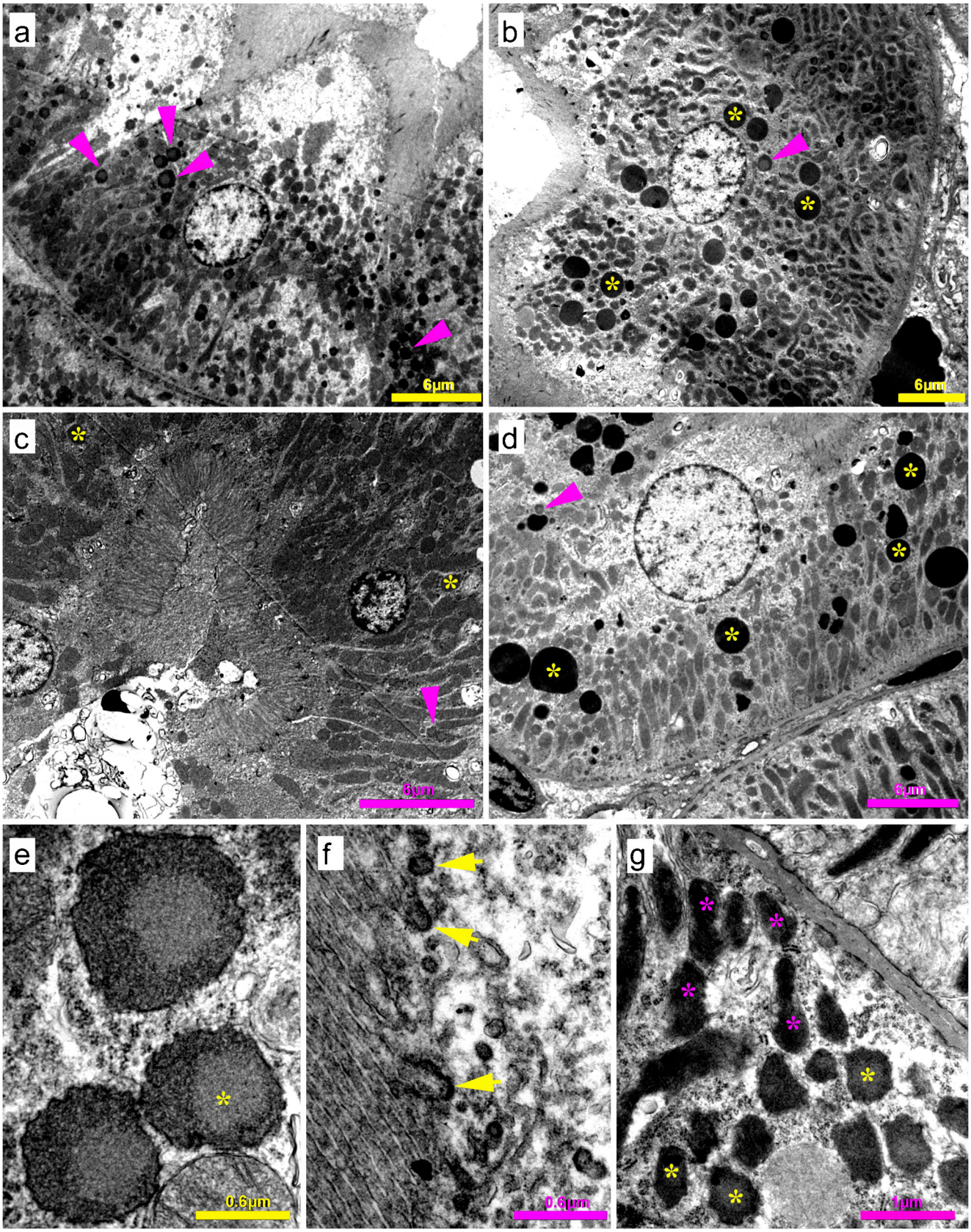

and STZ-N6 groups. Our findings are in agreement with numerous human and experimental studies that point out to the connection between ectopic lipid accumulation in the kidney and diabetes (Sun et al. 2002; Wang et al. 2005;

◀ **Fig. 9** Transmission electron microscopy (TEM) microphotographs of the proximal tubules stained for VEGF. Representative TEM microphotographs of the proximal tubules (**a**–**f**). (**a**) PTCs from control group (C group) had many VEGF-immunoreactive vesicles (examples are indicated by pink arrowheads) in cytoplasm, confirming the finding from immunofluorescent light microscopy. (**b**) In kidneys from DM1 group (STZ), VEGF-immunoreactive vesicles were still present, but they were lesser in number. There were many lipid droplets (LDs; examples are indicated by yellow asterisk) in cytoplasm, which were larger in comparison to the vesicles and had very high electron density. (**c**) Cytoplasm of the PTCs in DM1 group fed with n−6/n−3 ratio of 0.05 (16% EPA and 19% DHA; STZ + DHA) contained LDs, while VEGF-immunoreactive vesicles were very rare. (**d**) In cytoplasm of the PTCs of DM1 group fed with n−6/n−3 ratio of 60 (STZ + N6), many large LDs were found along with rare VEGF-immunoreactive vesicles. (**e**) High-power magnification has shown appearance of the VEGF-immunoreactive vesicles in control rat. VEGF immunoreactivity was condensated on the superficial parts of the vesicles and their membrane. (**f**) A detail of endocytotic vesicle formation (arrows) at the base of the brush border of PTC's apical membrane, showing strong VEGF immunoreactivity. (**g**) High-power magnification shows damaged mitochondria (pink asterisk) and deformed endocytotic vesicles (yellow asterisk) in PTC of diabetic rat

Herman-Edelstein et al. 2013; Proctor et al. 2006; Ishizaka et al. 2010; Yuan et al. 2017).

The presumed mechanisms which underlie lipid accumulation in the kidney include increased activity of SREPB-1 and -2 with increased expression of fatty acid synthase and acetyl CoA carboxylase (Sun et al. 2002; Wang et al. 2005; Jun et al. 2009); upregulation of pathways involved in tubular reabsorption of filtered protein-bound lipids via the megalin–cubilin complex; increased glucose load per nephron; influx of oxidized lipoproteins (Kim et al. 2009); increased uptake of fatty acids carried on filtered albumin by the renal tubules due to the increased urinary excretion of albumin (Thomas et al. 1995); as well as disruption of intercellular cholesterol feedback regulation by advanced glycation end-products (AGE) Yuan et al. 2017). Long-chain fatty acids (LCFA) act as ligands of peroxisome proliferator-activated receptors (Nakamura et al. 2013), which, in turn, regulate lipid storage (Schoonjans et al. 1996). In addition, PUFA, but not SFA or MUFA, suppress the induction of lipogenic genes by inhibiting the expression and processing of SREBP-1c (Nakamura et al. 2005).

Among LCFA, EPA and DHA have previously been shown to suppress formation of lipid droplets and fat storage in lipid droplets (Manickam et al. 2010; Barber et al. 2013). This could be an explanation for the lower extent of lipid accumulation that we found in PTCs of n−3-supplemented, in comparison to normally fed and n−6-supplemented diabetic rats.

Finally, we also studied the expression pattern of VEGF protein in PTCs. We did not find significant changes in VEGF protein expression, according to our Western blot results. This was in agreement with strong VEGF expression in podocytes that we observed by using TEM. However, we found dramatic changes in expression pattern profiles of VEGF in PTCs. Kidneys of the control group of rats showed higher number of proximal tubules with VEGF-immunoreactive granules in the cytoplasm. In all the other groups of animals, to which was given streptozotocin, pattern of VEGF immunofluorescence was completely changed and granular form was observed only occasionally in the kidney sections from the STZ group. In our previous work, in a DM type 2 model, during prolonged hyperglycaemia, we found dynamic redistribution of VEGF in proximal tubular cells with VEGF present in vesicular apparatus of normal rat kidney and its translocation to the apical membrane of PTC in a sucrose-damaged renal tissue, which led us to the conclusion that VEGF is using the endocytotic trafficking system to be re-absorbed in PTCs (Vitlov Uljevic et al. 2018).

Our present data indicate that vesicular trafficking in the PTC system was damaged in DM1. Fatty acids have important role in membrane order, lipid raft structure and function and membrane trafficking. Dietary n−3 PUFA are incorporated in various cell types (Fan et al. 2004) altering the biochemical content of membrane lipid microdomains, which may influence membrane fusion and protein trafficking (Ma et al. 2004; Seo et al. 2006). In our study, we found that PUFA supplementation did not help in restoring of vesicular VEGF transport damaged by DM1. Moreover, on a base of the absence of VEGF-immunoreactive vesicles as well as the ultrastructural findings, we believe that n−3 and n−6 supplementation, in diabetic conditions, resulted in greater instability of endocytotic vesicles.

In summary, our data have shown substantial influence of DM1 and dietary PUFA lipid content on renal phospholipid fatty acid composition. These changes were followed by dramatic vacuolization of distal tubular cells in DM1, which was diminished in n−3 PUFA-supplemented rats. Processes of DTC vacuolization were followed by higher expression of SATB1 in DTCs, particularly in diabetic animals supplemented with n−6 and n−3 PUFAs. The ectopic lipid accumulation was found in PTCs of all diabetic animals, but it was worsened in rats receiving n−6 PUFA supplementation. In addition, in DM1, we found disturbance in the VEGF-transporting vesicular PTC system, which was substantially worsened by n−6 and n−3 PUFA supplementation. According to our findings, SATB1 could be considered as a histological marker for the distal tubular cell damage. We concluded that the role of DTC damage in early phase of DN has been widely underestimated and that dietary fatty acid composition and PUFA supplementation can strongly influence the outcomes of DN, although their effects are not simply straightforward. More attention should be given by clinicians to the urgent treatment of hyperglycaemia in early phase of DM1, in order to prevent distal tubular cell damage and its further complications.

Acknowledgements This work has been supported in part by the Croatian Science Foundation under the projects (IP-2014-09-8992; T. Mašek and 3163; K. Starčević) and by the Ministry of Science, Education and Sports of the Republic of Croatia (I. Bočina, K. Vukojević, N. Filipović).

Compliance with ethical statements

Conflict of interest On behalf of all the authors, the corresponding author states that there is no conflict of interest.

Ethical approval All applicable international, national and/or institutional guidelines for the care and use of animals were followed. All experimental protocols were approved by the National Ethics Committee (EP 13/2015) and Veterinary Directorate, Ministry of Agriculture, Republic of Croatia and conducted according to the Croatian Animal Welfare Act.

References

Agnic I, Vukojevic K, Saraga-Babic M, Filipovic N, Grkovic I (2013) Isoflurane post-conditioning stimulates the proliferative phase of myocardial recovery in an ischemia-reperfusion model of heart injury in rats. Histol Histopathol 29:89–99

Alvarez JD, Yasui DH, Niida H, Joh T, Loh DY, Kohwi-Shigematsu T (2000) The MAR-binding protein SATB1 orchestrates temporal and spatial expression of multiple genes during T-cell development. Genes Dev 14:521–535

Bang HO, Dyerberg J, Hjoorne N (1976) The composition of food consumed by Greenland Eskimos. Acta Med Scand 200:69–73

Barber E, Sinclair AJ, Cameron-Smith D (2013) Comparative actions of omega-3 fatty acids on in-vitro lipid droplet formation. Prostaglandins Leukot Essent Fatty Acids 89:359–366

Barcelli UO, Weiss M, Beach D, Motz A, Thompson B (1990) High linoleic acid diets ameliorate diabetic nephropathy in rats. Am J Kidney Dis 16:244–251

Blantz RC, Singh P (2014) Glomerular and tubular function in the diabetic kidney. Adv Chronic Kidney Dis 21(3):297–303 Epub 2014/05/02

Calder PC (2007) Immunomodulation by omega-3 fatty acids. Prostaglandins Leukot Essent Fatty Acids. 77:327–335

Delic Jukic IK, Kostic S, Filipovic N, Gudelj Ensor L, Ivandic M, Dukic JJ, Vitlov Uljevic M, Ferhatovic Hamzic L, Puljak L, Vukojevic K (2018) Changes in expression of special AT-rich sequence binding protein 1 and phosphatase and tensin homologue in kidneys of diabetic rats during ageing. Nephrol Dial Transplant 33:1075

Di Stasi D, Bernasconi R, Marchioli R, Marfisi RM, Rossi G, Tognoni G, Tacconi MT (2004) Early modifications of fatty acid composition in plasma phospholipids, platelets and mononucleates of healthy volunteers after low doses of n-3 polyunsaturated fatty acids. Eur J Clin Pharmacol 60:183–190

Fan YY, Ly LH, Barhoumi R, McMurray DN, Chapkin RS (2004) Dietary docosahexaenoic acid suppresses T cell protein kinase C theta lipid raft recruitment and IL-2 production. J Immunol 173: 6151–6160

Ferrara N (1999) Role of vascular endothelial growth factor in the regulation of angiogenesis. Kidney Int 56:794–814

Folch J, Lees M, Sloane Stanley GH (1957) A simple method for the isolation and purification of total lipides from animal tissues. J Biol Chem 226:497–509

Fujikawa M, Yamazaki K, Hamazaki T, Wakaki K, Koizumi F, Yano S, Kobayashi M (1994) Effect of eicosapentaenoic acid ethyl ester on albuminuria in streptozotocin-induced diabetic rats. J Nutr Sci Vitaminol (Tokyo) 40:49–61

Garman JH, Mulroney S, Manigrasso M, Flynn E, Maric C (2009) Omega-3 fatty acid rich diet prevents diabetic renal disease. Am J Physiol Renal Physiol. 296:F306–F316

Gilbert RE (2017) Proximal tubulopathy: prime mover and key therapeutic target in diabetic kidney disease. Diabetes 66:791–800

Hamazaki T, Takazakura E, Osawa K, Urakaze M, Yano S (1990) Reduction in microalbuminuria in diabetics by eicosapentaenoic acid ethyl ester. Lipids 25:541–545

Herman-Edelstein M, Scherzer P, Tobar A, Levi M, Gafter U (2013) Altered renal lipid metabolism and renal lipid accumulation in human diabetic nephropathy. J Lipid Res 55:561–572

Holman RT, Johnson SB, Gerrard JM, Mauer SM, Kupcho-Sandberg S, Brown DM (1983) Arachidonic acid deficiency in streptozotocin-induced diabetes. Proc Natl Acad Sci U S A 80:2375–2379

Horrocks LA, Yeo YK (1999) Health benefits of docosahexaenoic acid (DHA). Pharmacol Res 40:211–225

Ibrahim W, Lee US, Szabo J, Bruckner G, Chow CK (1999) Oxidative stress and antioxidant status in mouse kidney: effects of dietary lipid and vitamin E plus iron. J Nutr Biochem 10:674–678

Ishizaka N, Hongo M, Matsuzaki G, Furuta K, Saito K, Sakurai R, Sakamoto A, Koike K, Nagai R (2010) Effects of the AT(1) receptor blocker losartan and the calcium channel blocker benidipine on the accumulation of lipids in the kidney of a rat model of metabolic syndrome. Hypertens Res 33:263–268

Jun H, Song Z, Chen W, Zanhua R, Yonghong S, Shuxia L, Huijun D (2009) In vivo and in vitro effects of SREBP-1 on diabetic renal tubular lipid accumulation and RNAi-mediated gene silencing study. Histochem Cell Biol 131:327–345

Kim HJ, Moradi H, Yuan J, Norris K, Vaziri ND (2009) Renal mass reduction results in accumulation of lipids and dysregulation of lipid regulatory proteins in the remnant kidney. Am J Physiol Renal Physiol 296:F1297–F1306

Lawrence T (2009) The nuclear factor NF-kappaB pathway in inflammation. Cold Spring Harb Perspect Biol 1:a001651

Liu J, Yeo HC, Doniger SJ, Ames BN (1997) Assay of aldehydes from lipid peroxidation: gas chromatography-mass spectrometry compared to thiobarbituric acid. Anal Biochem 245:161–166

Ma DW, Seo J, Switzer KC, Fan YY, McMurray DN, Lupton JR, Chapkin RS (2004) n-3 PUFA and membrane microdomains: a new frontier in bioactive lipid research. J Nutr Biochem 15:700–706

Majumder S, Advani A (2016) VEGF and the diabetic kidney: more than too much of a good thing. J Diabetes Complicat 31:273–279

Manickam E, Sinclair AJ, Cameron-Smith D (2010) Suppressive actions of eicosapentaenoic acid on lipid droplet formation in 3T3-L1 adipocytes. Lipids Health Dis 9:57

Masek T, Filipovic N, Hamzic LF, Puljak L, Starcevic K (2014) Long-term streptozotocin diabetes impairs arachidonic and docosahexaenoic acid metabolism and 5 desaturation indices in aged rats. Exp Gerontol 60:140–146

Masek T, Filipovic N, Vuica A, Starcevic K (2017) Effects of treatment with sucrose in drinking water on liver histology, lipogenesis and lipogenic gene expression in rats fed high-fiber diet. Prostaglandins Leukot Essent Fatty Acids 116:1–8

Mollsten AV, Dahlquist GG, Stattin EL, Rudberg S (2001) Higher intakes of fish protein are related to a lower risk of microalbuminuria in young Swedish type 1 diabetic patients. Diabetes Care 24:805–810

Mora-Fernandez C, Dominguez-Pimentel V, de Fuentes MM, Gorriz JL, Martinez-Castelao A, Navarro-Gonzalez JF (2014) Diabetic kidney disease: from physiology to therapeutics. J Physiol 592:3997–4012

Nakamura MT, Cheon Y, Li Y, Nara TY (2005) Mechanisms of regulation of gene expression by fatty acids. Lipids 39:1077–1083

Nakamura MT, Yudell BE, Loor JJ (2013) Regulation of energy metabolism by long-chain fatty acids. Prog Lipid Res 53:124–144

Paton CM, Ntambi JM (2010) Loss of stearoyl-CoA desaturase activity leads to free cholesterol synthesis through increased Xbp-1 splicing. Am J Physiol Endocrinol Metab 299:E1066–E1075

Patterson E, Wall R, Fitzgerald GF, Ross RP, Stanton C (2012) Health implications of high dietary omega-6 polyunsaturated fatty acids. J Nutr Metab 2012:539426

Pinnamaneni SK, Southgate RJ, Febbraio MA, Watt MJ (2006) Stearoyl CoA desaturase 1 is elevated in obesity but protects against fatty acid-induced skeletal muscle insulin resistance in vitro. Diabetologia 49:3027–3037

Proctor G, Jiang T, Iwahashi M, Wang Z, Li J, Levi M (2006) Regulation of renal fatty acid and cholesterol metabolism, inflammation, and fibrosis in Akita and OVE26 mice with type 1 diabetes. Diabetes 55: 2502–2529

Satirapoj B (2013) Nephropathy in diabetes. Adv Exp Med Biol 771: 107–122

Schmitz G, Ecker J (2008) The opposing effects of n-3 and n-6 fatty acids. Prog Lipid Res 47:147–155

Schoonjans K, Staels B, Auwerx J (1996) The peroxisome proliferator activated receptors (PPARS) and their effects on lipid metabolism and adipocyte differentiation. Biochim Biophys Acta 1302:93–109

Seo J, Barhoumi R, Johnson AE, Lupton JR, Chapkin RS (2006) Docosahexaenoic acid selectively inhibits plasma membrane targeting of lipidated proteins. FASEB J 20:770–772

Shapiro H, Theilla M, Attal-Singer J, Singer P (2010) Effects of polyunsaturated fatty acid consumption in diabetic nephropathy. Nat Rev Nephrol 7:110–121

Shimizu H, Ohtani K, Tanaka Y, Sato N, Mori M, Shimomura Y (1995) Long-term effect of eicosapentaenoic acid ethyl (EPA-E) on albuminuria of non-insulin dependent diabetic patients. Diabetes Res Clin Pract 28:35–40

Shoji T, Kakiya R, Hayashi T, Tsujimoto Y, Sonoda M, Shima H et al (2013) Serum n-3 and n-6 polyunsaturated fatty acid profile as an independent predictor of cardiovascular events in hemodialysis patients. Am J Kidney Dis 62:568–576

Simopoulos AP (1997) Omega-3 fatty acids in the prevention-management of cardiovascular disease. Can J Physiol Pharmacol 75:234–239

Simopoulos AP (2009) Evolutionary aspects of the dietary omega-6:omega-3 fatty acid ratio: medical implications. World Rev Nutr Diet 100: 1–21

Starcevic K, Filipovic N, Galan A, Micek V, Gudan Kurilj A, Masek T (2018) Hepatic lipogenesis and brain fatty acid profile in response to different dietary n6/n3 ratios and DHA/EPA supplementation in streptozotocin treated rats. Mol Nutr Food Res 62:e1701007

Sun L, Halaihel N, Zhang W, Rogers T, Levi M (2002) Role of sterol regulatory element-binding protein 1 in regulation of renal lipid metabolism and glomerulosclerosis in diabetes mellitus. J Biol Chem 277:18919–18927

Takahashi M, Ando J, Shimada K, Nishizaki Y, Tani S, Ogawa T, Yamamoto M, Nagao K, Hirayama A, Yoshimura M, Daida H, Nagai R, Komuro I (2017) The ratio of serum n-3 to n-6 polyunsaturated fatty acids is associated with diabetes mellitus in patients with prior myocardial infarction: a multicenter cross-sectional study. BMC Cardiovasc Disord 17:41

Thomas ME, Morrison AR, Schreiner GF (1995) Metabolic effects of fatty acid-bearing albumin on a proximal tubule cell line. Am J Phys 268:F1177–F1184

Tosi F, Sartori F, Guarini P, Olivieri O, Martinelli N (2014) Delta-5 and delta-6 desaturases: crucial enzymes in polyunsaturated fatty acid-related pathways with pleiotropic influences in health and disease. Adv Exp Med Biol 824:61–81

Vitlov Uljevic M, Bocina I, Restovic I, Kunac N, Masek T, Kretzschmar G, Grobe M, Saric M, Vukojevic K, Saraga-Babic M, Filipovic N (2018) Reabsorption in the proximal tubuli-ultrastructural evidence for a novel aspect of renal VEGF trafficking. Cell Tissue Res 374: 189–201

Vuica A, Ferhatovic Hamzic L, Vukojevic K, Jeric M, Puljak L, Grkovic I, Filipovic N (2015) Aging and a long-term diabetes mellitus increase expression of 1 alpha-hydroxylase and vitamin D receptors in the rat liver. Exp Gerontol 72:167–176

Wang Z, Jiang T, Li J, Proctor G, McManaman JL, Lucia S, Chua S, Levi M (2005) Regulation of renal lipid metabolism, lipid accumulation, and glomerulosclerosis in FVBdb/db mice with type 2 diabetes. Diabetes 54:2328–2335

Yabuki A, Tahara T, Taniguchi K, Matsumoto M, Suzuki S (2006) Neuronal nitric oxide synthase and cyclooxygenase-2 in diabetic nephropathy of type 2 diabetic OLETF rats. Exp Anim 55:17–25

Yilmaz O, Ozkan Y, Yildirim M, Ozturk AI, Ersan Y (2002) Effects of alpha lipoic acid, ascorbic acid-6-palmitate, and fish oil on the glutathione, malonaldehyde, and fatty acids levels in erythrocytes of streptozotocin induced diabetic male rats. J Cell Biochem 86:530–539

Yin H, Xu L, Porter NA (2011) Free radical lipid peroxidation: mechanisms and analysis. Chem Rev 111:5944–5972

Yokoyama M, Origasa H, Matsuzaki M, Matsuzawa Y, Saito Y, Ishikawa Y, Oikawa S, Sasaki J, Hishida H, Itakura H, Kita T, Kitabatake A, Nakaya N, Sakata T, Shimada K, Shirato K (2007) Effects of eicosapentaenoic acid on major coronary events in hypercholesterolaemic patients (JELIS): a randomised open-label, blinded endpoint analysis. Lancet 369:1090–1098

Yuan Y, Sun H, Sun Z (2017) Advanced glycation end products (AGEs) increase renal lipid accumulation: a pathogenic factor of diabetic nephropathy (DN). Lipids Health Dis 16:126

Zhang S, Gao X, Ma Y, Jiang J, Dai Z, Yin X, Min W, Hui W, Wang B (2015) Expression and significance of SATB1 in the development of breast cancer. Genet Mol Res 14:3309–3317